AUTHOR QUERY FORM

ELSEVIER	**Journal: CSTE** **Article Number: 4652**	**Please e-mail or fax your responses and any corrections to:** **E-mail: corrections.esch@elsevier.sps.co.in** **Fax: +31 2048 52799**

Dear Author,

Any queries or remarks that have arisen during the processing of your manuscript are listed below and highlighted by flags in the proof. Please check your proof carefully and mark all corrections at the appropriate place in the proof (e.g., by using on-screen annotation in the PDF file) or compile them in a separate list.

For correction or revision of any artwork, please consult http://www.elsevier.com/artworkinstructions.

Articles in Special Issues: Please ensure that the words 'this issue' are added (in the list and text) to any references to other articles in this Special Issue.

Uncited references: References that occur in the reference list but not in the text – please position each reference in the text or delete it from the list.

Missing references: References listed below were noted in the text but are missing from the reference list – please make the list complete or remove the references from the text.

Location in article	Query / remark Please insert your reply or correction at the corresponding line in the proof
	No Queries

Electronic file usage
Sometimes we are unable to process the electronic file of your article and/or artwork. If this is the case, we have proceeded by:

☐ Scanning (parts of) your article ☐ Rekeying (parts of) your article ☐ Scanning the artwork

Thank you for your assistance.

Composites Science and Technology xxx (2010) xxx–xxx

Contents lists available at ScienceDirect

Composites Science and Technology

journal homepage: www.elsevier.com/locate/compscitech

Characterization of epoxy functionalized graphite nanoparticles and the physical properties of epoxy matrix nanocomposites

Sandi G. Miller [a,*], Jonathan L. Bauer [b], Michael J. Maryanski [c], Paula J. Heimann [d], Jeremy P. Barlow [e], Jan-Michael Gosau [e], Ronald E. Allred [e]

[a] Polymers Branch, NASA Glenn Research Center, Cleveland, OH 44135, United States
[b] Department of Chemical Engineering, University of Michigan, Ann Arbor, MI 48109, United States
[c] Department of Chemical Engineering, University of Akron, Akron, OH 44325, United States
[d] Ohio Aerospace Institute, Cleveland, OH 44135, United States
[e] Adherent Technologies, Inc., Albuquerque, NM 87111, United States

ARTICLE INFO

Article history:
Received 8 May 2009
Received in revised form 10 February 2010
Accepted 24 February 2010
Available online xxxx

Keywords:
A. Nanocomposites
A. Polymer
B. Electrical properties
B. Mechanical properties

ABSTRACT

This work presents a novel approach to the functionalization of graphite nanoparticles. The technique provides a mechanism for covalent bonding between the filler and matrix, with minimal disruption to the sp^2 hybridization of the pristine graphene sheet. Functionalization proceeded by covalently bonding an epoxy monomer to the surface of expanded graphite, via a coupling agent, such that the epoxy concentration was measured as approximately 4 wt.%. The impact of dispersing this material into an epoxy resin was evaluated with respect to the mechanical properties and electrical conductivity of the graphite–epoxy nanocomposite. At a loading as low as 0.5 wt.%, the electrical conductivity was increased by five orders of magnitude relative to the base resin. The material yield strength was increased by 30% and Young's modulus by 50%. These results were realized without compromise to the resin toughness.

1. Introduction

As advanced materials applications dictate increasingly rigorous composite performance, innovative technologies capable of providing properties beyond those of traditional polymer matrix composites are becoming necessary. Recently, multi-functional composites providing structural integrity, as well as imparting additional capabilities have been widely investigated [1,2]. Nanomaterials in particular have been called upon to provide such performance.

Nanoparticulate fillers enable property enhancement as a result of the large interface available to the matrix [3,4] This interfacial area is only beneficial however, if matrix and particle contact is optimized. Several techniques to modify nanoparticle surfaces have been identified, and vary, based on the particulate chemistry. For example, layered silicate clays are typically made compatible with a matrix by exchange of the naturally occurring inorganic cation within the silicate with a positively charged organic compound [5]. Carbon nanotubes have been modified by oxidation of the tube [6–8], by covalently bonding an organic functionality to the tube [9–11], or by non-covalent methods [12,13]. Graphite nanoflakes are often functionalized through processes beginning with oxidation of the graphene plane [14–16], or by a coating and compounding method developed by the Drzal group [17]. In most cases, chemical modification results in material property trade-offs; for example, functionalization may improve dispersion, however, functionalization of carbon particles can compromise conductivity [18–20].

Graphene platelets, in their pristine form, are characterized by a low surface energy, and are therefore poorly wetted by most polymer matrices. Consequently, dispersion is often poor, leading to reduced mechanical properties of the composite. However, the aromatic nature of the un-oxidized graphene planes offer greatly enhanced transport properties, such as thermal and electrical conductivity. Such potential is reached when the graphene sheets are dispersed into individual platelets, which again is difficult in a situation where wetting is poor. Therefore, oxidation and functionalization is necessary to improve dispersion, however this occurs with the risk of reducing conductivity. There have been recent publications which address tailoring nanocomposite properties using graphene sheets oxidized to various extents to mitigate the trade-off between mechanical and transport properties [21,22]. The functionalization technique described in this work does not begin with oxidation. Rather, an epoxy monomer was covalently bonded to the graphite surface through a coupling agent. This provided a means to create a strong filler matrix interface without significant impact to the conductivity.

* Corresponding author. Tel.: +1 216 433 8489; fax: +1 216 977 7132.
E-mail address: Sandi.G.Miller@nasa.gov (S.G. Miller).

0266-3538/$ - see front matter © 2010 Published by Elsevier Ltd.
doi:10.1016/j.compscitech.2010.02.023

2. Experimental

2.1. Materials

Epoxy resin, Epon 826, was generously supplied by Resolution Performance Products. Araldite DY3601, an aliphatic epoxy resin, and Jeffamine D230 curing agent were supplied by Huntsman Chemicals. TG-679 is a Graftech product which was chemically modified by Adherent Technologies, and the epoxy modified version of this graphite will be referred to as ATI graphite [23,24]. Untreated expanded graphite from Superior Graphite was used for comparison, and will be referred to as EG.

2.2. ATI preparation

Expanded graphite, TG-679, (10.0 g) was combined with ATI-9307 coupling agent (0.01 g) in 50 mL of 2-butanone (MEK). The mixture was allowed to stir for 20 min to ensure homogeneity. The solvent was then removed by rotary evaporation. The treated graphite was combined with EPON 828 (0.10 g) in 50 mL CH_2Cl_2. The mixture was allowed to stir for 20 min, and the solvent was removed by rotary evaporation. The graphite was then placed under vacuum at 50 °C to remove residual solvent. To activate the coupling agent, the graphite was heated in a vented oven at 210 °C for 20 min. Once cool, the graphite was placed in an amber vial and purged with argon. The particle dimensions of this material were on the order of 50 μm in the lateral dimensions whereas the lateral dimensions of expanded graphites (EG) have a typical range of 300–900 μm (UCAR Grafguard 160–50A). The quantity of epoxy coverage was characterized by TGA to equal approximately 4 wt.%.

The TGA characterization of ATI nanoparticles proceeded by collecting an initial TGA curve of the ATI particles. The TGA curve of as-received ATI graphite showed a weight loss of approximately 4%, before the material rapidly degraded above 600 °C. That weight loss was attributed to the epoxy functionality covalently coupled to the graphite. This was confirmed through reaction of methylene dianiline (MDA) to the epoxy functionalized graphite. The ATI nanoparticles (0.5 g) were dispersed in distilled water (85 mL) at room temperature, under nitrogen flow. MDA (1.5 g, 7.6 mmol) was dissolved in 25 mL ethanol. The MDA/ethanol solution was added drop-wise to the aqueous suspension under vigorous stirring. The mixture stirred for 24 h. The modified graphite was dried, washed repeatedly with warm ethanol, and dried in a vacuum oven overnight at 90 °C. These materials were characterized by TGA to calculate the amount of MDA that had been grafted to each material.

Following this reaction, the TGA curve showed ~8% weight loss between 240 °C and 600 °C, before rapid degradation, again above 600 °C. This result indicated that MDA is present in 4% by weight of the sample, or 0.22 mmol MDA per 1 g of ATI graphite.

2.3. Nanocomposite preparation

Resin plaques of Epon 826 and DY3601 epoxy blends were prepared in 70:30 equivalent epoxy ratios with graphite content of 0.5 wt.% and 1.0 wt.%. Epon 826 (18.4 g), DY3601 (7.875 g), and the calculated amount of graphite were mixed at room temperature for 4 h. The curing agent, D230 (7.5 g), was added to the mixture and poured into a 10.2 cm by 10.2 cm mold. The resin was degassed at 40 °C for 3 h then cured at 75 °C and 125 °C for 2 h each. The preparation of nanocomposites prepared with excess amine curing agent followed the above procedure, using 7.9 g D230 curing agent, 5% excess amine, or 8.25 g D230, 10% excess amine.

2.4. Characterization

X-ray diffraction (XRD) patterns were obtained using a Philips XRG 3100 X-ray diffractometer with Ni-filtered Cu Kα radiation. The XRD data was recorded in the range of $2\theta = 2–32°$.

Transmission electron microscopy (TEM) specimens were prepared by microtoming nanocomposite samples, 20–70 nm thick, and floating the sections onto Cu grids. Micrographs were obtained with a Philips CM 200, using an acceleration voltage of 200 kV. The TEM images shown throughout this work are representative of the dispersion observed throughout several sections, taken from various regions, of each nanocomposite sample.

Electrical conductivity measurements were made by cutting samples of approximately 3.5 cm by 0.7 cm from larger preparative composites. Silver paint was used to apply electrical contacts to the ends of the sample, covering top, bottom, sides, and end. The thickness, width, and length dimensions of the composite were measured using a digital micrometer. The length used for calculations was the gauge length between the electrodes. The samples were mounted using spring clips into a Keithley Model 8002 Restest High Resistance Test Box to minimize stray currents. A constant voltage of 100.0 V dc was applied across the sample and current was measured using a Keithley Model 617 Electrometer.

Tensile tests were run according to ASTM D638. Three dog bone specimens of each material were tested. The tests were performed on MTS 800 instrument at a displacement rate of 1.40 cm per minute, using a 2200 N load cell. Optical measurements using digital image correlation, as opposed to strain gages, were made using ARAMIS software. In image correlation, a random speckle pattern is painted onto the specimen. Cameras then track the displacements of the speckled dots, and displacement fields and strains are calculated by specialized computer algorithms. Once calibrated, the software can measure specimens under loading and output strain and displacement results through automated methods without user intervention being required [25].

X-ray photoelectron spectroscopy samples were analyzed on a VG Mk II ESCALAB, using Mg Kα X-rays at 300 W. The system consisted of a turbo pumped prep chamber (base pressure 10^{-9} torr), a fast load entry lock; and a main chamber which maintained a base pressure of 1×10^{-10} torr using a diffusion pump with a cold trap. The spectra were taken with the surface plane normal to the analyzer axis (90° take off angle) using an aperture of 1 mm × 1 mm. Survey scans were initially taken to identify all components, followed by higher resolution individual region scans using a pass energy of 20 eV. The spectrometer was calibrated to yield the standard values of 75.13 eV for Cu3p and 932.66 eV for $Cu2p_{3/2}$. Atomic concentrations were then calculated based on the individual regions.

Viscosity measurements were performed by mixing graphite with the epoxy matrix at room temperature for times ranging from 15 min to 2 h. Viscosity data was collected by submerging the tip of a hand held Brookfield Synchro-lectric Viscometer into the resin and graphite mixture, and reading the measured viscosity. The viscosity is a measure of resistance to rotation of the viscometer tip.

3. Results and discussion

3.1. Characterization and dispersion of ATI graphite

ATI epoxy functionalized graphite was prepared using an expanded graphite precursor. The preparation of expanded graphite typically proceeds by acid intercalation of natural flake graphite, followed by rapid heating in an oven which has been preheated to approximately 1100 °C. At such temperatures, the acid quickly volatilizes and forces the graphite layers apart as it evaporates

Please cite this article in press as: Miller SG et al. Characterization of epoxy functionalized graphite nanoparticles and the physical properties of epoxy matrix nanocomposites. Compos Sci Technol (2010), doi:10.1016/j.compscitech.2010.02.023

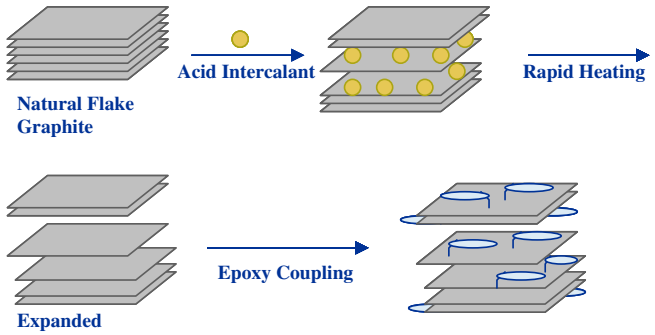

Fig. 1. Schematic of graphite expansion and functionalization process.

Table 1
Chemical characterization of graphite particles.

Sample	Density (g/cm^3)	XPS (% oxygen)	FTIR
EG	2.25	1	3600 cm^{-1} (OH-stretch) 1700 cm^{-1} (C=O stretch)
ATI-epoxy functionalized	1.7	9	3300 cm^{-1} (weak, OH-stretch) 2900, 2800 cm^{-1} (C–H stretch) 1700 cm^{-1} (C=O stretch) 1100 cm^{-1} (C–O/C–O–C stretch)

from within the graphite structure. The expansion process however does not expand each individual layer, but rather aggregates composed of several graphene planes are stacked in an expanded graphite "worm" [22].

The functionalization technique described in this work chemically modified only the outermost sheets of the stacked aggregates. As such, the material was functionalized to an extent, but several graphene planes remained in their pristine form. A schematic of this process is illustrated in Fig. 1, and the presence of such aggregates was confirmed using XRD as an intense diffraction peak at $2\theta = 26.7°$, corresponding to the d_{002} spacing of natural flake graphite.

The presence of the epoxy coating was confirmed by several techniques, as described in Table 1.

The density of the ATI epoxy functionalized graphite decreased, relative to the starting material, which indicated a change in the physical characteristics of the modified graphite. This was attributed to a reduction in particle size relative to the pristine expanded graphite. The increase in oxygen content, as measured by XPS and the appearance of IR bands corresponding to epoxy functionalities provide further confirmation of successful graphite modification. The SEM images in Fig. 2 shows the graphene surface before and after reaction with epoxy. The image in Fig. 2a is representative of the sharp crystalline surface of the graphite plane and the image in Fig. 2b shows that surface covered by the amorphous epoxy functionalization.

The extent of epoxy coverage was determined by TGA as approximately 4 wt.%. At this level of functionalization, a significant benefit to the graphite dispersion was observed within an epoxy matrix. TEM images presented in Fig. 3 illustrates the difference by which ATI functionalized graphite and expanded graphite were dispersed. The image in Fig. 3a is representative of the dispersion of expanded graphite within the epoxy matrix, where the black lines are the graphene plane edge. The image shows several graphene aggregates clustered in one region of the image. This unfunctionalized material was generally difficult to disperse by the methods used in this work and the result was aggregates of graphene sheets and clusters of those aggregates. Functionalization of the expanded graphite resulted in a considerably improved level of dispersion. Fig. 3b is a representative TEM image of ATI graphite/epoxy. In this case, the sheet edges are visible throughout most of the image. While some aggregation remains, the image shows a significant portion of the graphite dispersed into separate sheets. Additionally, overlap of the separate layers is visible in Fig. 3b. The layer overlap contributes to the low graphite loading required to measure electrical conductivity in this material. The nanocomposite conductivity will be discussed in greater detail later in this paper.

The improvement in dispersion was due, in part, to the functionalization present on some ATI graphite layers. However, it may also have been a result of the decreased ATI graphite particle size. The particle size of the ATI material was reported by the manufacturer as 50 μm, vs. initial starting size of hundreds of microns for the EG material.

The viscosity of each nanocomposite was measured during graphite dispersion to understand the influence that reduced particle size and functionalization may have had on the dispersion process. The data is plotted in Fig. 4. The results demonstrate a significant increase in melt viscosity on mixing the unfunctionalized EG particles. Dispersion of the ATI functionalized particles also increased viscosity, relative to the unfilled resin, however the extent of that increase was 50% less than that of the EG, despite the greater volume of ATI graphite present in the matrix.

The dispersion mechanism of ATI graphite was of interest as the material was only partially functionalized. Therefore, while the outermost sheets of an aggregate may be relatively easily separated; there remain aggregates of unmodified, closely spaced graphene sheets. The reason for the decline in the viscosity on mixing the EG at 1.0 wt.% is unclear at this time and requires additional analysis.

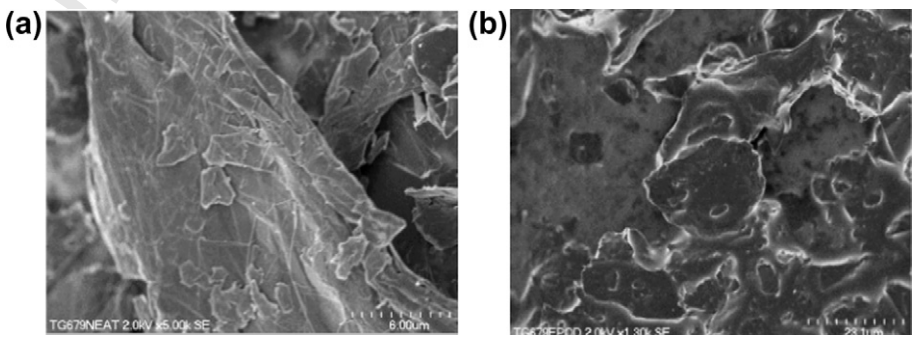

Fig. 2. SEM images of expanded graphite: (a) before and (b) after epoxy functionalization.

Please cite this article in press as: Miller SG et al. Characterization of epoxy functionalized graphite nanoparticles and the physical properties of epoxy matrix nanocomposites. Compos Sci Technol (2010), doi:10.1016/j.compscitech.2010.02.023

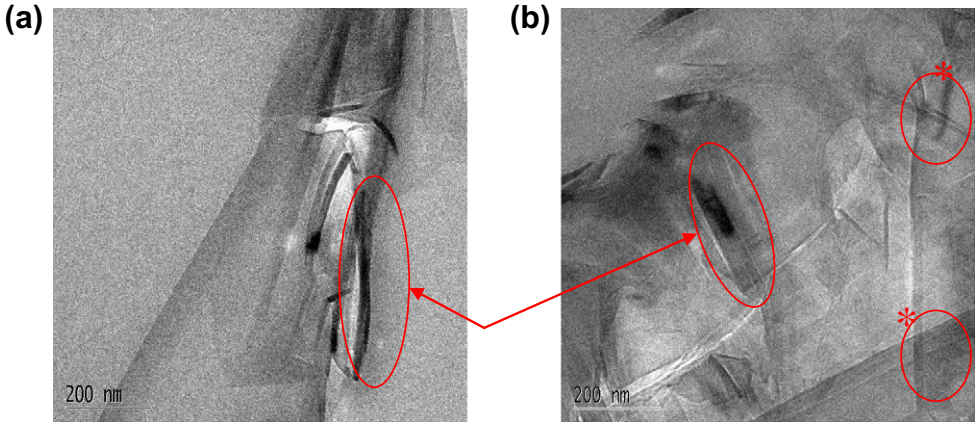

Fig. 3. TEM images of: (a) unfunctionalized and (b) functionalized graphite dispersed in an epoxy resin. Aggregated graphene sheets are represented by the circled dark lines, and the layer overlay in seen in Fig. 3b is circled and marked with an asterisk.

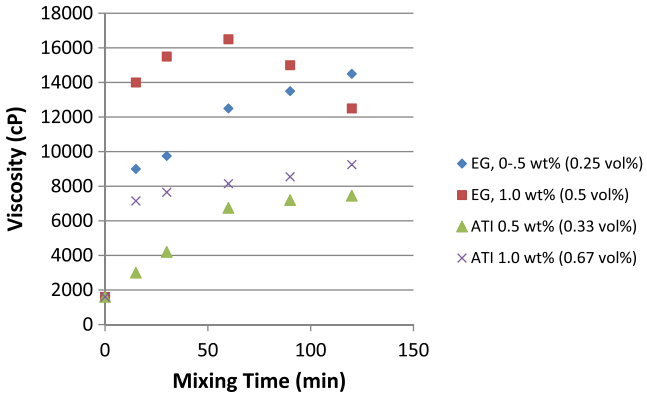

Fig. 4. Melt viscosity of epoxy/graphite during dispersion.

Dispersion was tracked by XRD as a function of mixing time. The XRD patterns of 1.0 wt.% ATI at increasing mixing times are shown in Fig. 5. The height of the diffraction peak cannot be used to quantify the number of aggregated graphene sheets as intensity is relative and varies from sample to sample. However, the presence of the diffraction peak does indicate that a number of graphene layers remain intact until mixing exceeds 15 min. The diffraction peak is absent for mixing times between 30 min and 2 h, as indicated as the flat lines in the plot. The XRD patterns suggested graphene exfoliation, or an undetectable degree of aggregation, beyond 15 min of mixing for both 1.0 and 0.5 wt.% percent ATI.

The dispersion times correspond well to the observed increase in viscosity. Within the first 15 min of mixing the resin and graphite, the viscosity doubled in the 0.5 wt.% material (from 1600 cP to 3000 cP), and increased by a factor of 4 in the 1.0 wt.% material (from 1600 cP to 7100 cP). An increase in viscosity would be expected as the graphene is dispersing and more graphene surface area is available for interaction with the matrix. Beyond 15 min, the viscosity continued to increase, as graphite separation continued, however the rate of viscosity increase slows at longer mixing times. This suggests that the majority of the layers are separated and in contact with the epoxy, as confirmed by the XRD pattern.

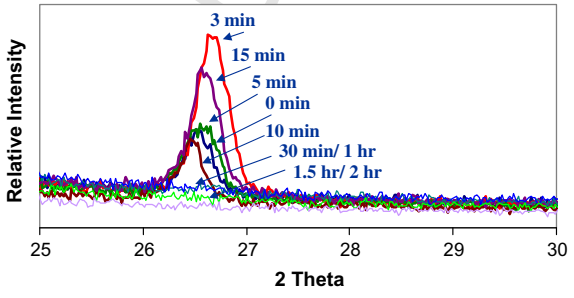

Fig. 5. XRD patterns of 0.5 wt.% ATI in epoxy at increased mixing times.

3.2. Electrical conductivity and mechanical properties

The interest of this paper was to evaluate trade-offs in mechanical and transport properties that may result from functionalization, taking into account the variation in dispersion between the unfunctionalized EG and ATI epoxy functionalized graphite. Both the mechanical properties and the conductivity were evaluated on samples where ATI graphite was added to a stoichiometric ratio of epoxy and curing agent. However, the presence of epoxy functionalities on the graphite holds the potential to disrupt matrix stoichometry, impacting material properties. Therefore, nanocomposite materials were also evaluated with either 5% or 10% excess amine curing agent. This introduced reactive functionalities that could bond between the filler and matrix.

3.2.1. Electrical conductivity

The conductivity of the nanocomposites increased with increasing graphite concentration, as listed in Table 2. The resistivity of the non-conductive pristine epoxy, was on the order of 5×10^{10} ohm-cm. ATI dispersion increased the conductivity by up to five orders of magnitude at 1.0 wt.% loading (0.67 vol.%). On the other hand, the unfunctionalized, but poorly dispersed EG required a 3 wt.% loading before percolation was reached. The low loading of ATI functionalized graphite required to improve conductivity by five orders of magnitude is comparable to, or an improvement of, the conductivity of many reported graphite–polymer composites [26–28]. With respect to graphite nanocompos-

Table 2
Electrical resistivity (R) data for epoxy containing EG or ATI graphite.

Graphite	R (ohm cm) 0.5 wt.%	R (ohm cm) 1.0 wt.%	R (ohm cm) 3.0 wt.%
EG	3.0E+10 (non-conductive)	1.0E+10 (non-conductive)	3.0E+8
ATI	1.3E+7	8.8E+5	
ATI (5% excess amine)	4.6E+6	1.4E+5	
ATI (10% excess amine)	2.2E+6	9.1E+5	

Please cite this article in press as: Miller SG et al. Characterization of epoxy functionalized graphite nanoparticles and the physical properties of epoxy matrix nanocomposites. Compos Sci Technol (2010), doi:10.1016/j.compscitech.2010.02.023

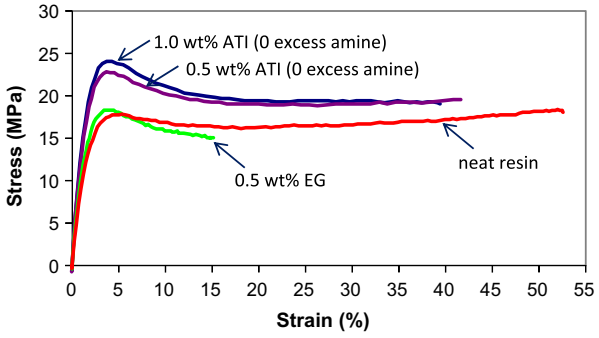

Fig. 6. Stress–strain curves of the neat epoxy, 0.5 wt.% EG, 0.5 wt.% ATI (0 excess amine), and 1.0 wt.% ATI (0 excess amine).

ites, the authors only found a lower percolation reported by Drzal, where a polymer coating and compounding technique was also used to disperse the graphite [17].

While poor dispersion will negatively impact conductivity by requiring high loading to reach percolation, extensive oxidation or functionalization may also lead to a non-conductive material [29,30]. The partial functionalization present on ATI graphite resulted in a level of dispersion and functionalization that was acceptable to reach percolation at a low loading. The exceptional improvement in electrical conductivity may be attributed to the presence of un-oxidized graphene layers within the material, as well as the layer overlap that was observed by TEM.

The addition of excess amine to this material did not impact the electrical conductivity of the material. The purpose of adding the excess amine was to improve upon the strength of the interface, therefore any influence would be expected in the mechanical properties.

3.2.2. Mechanical properties

Representative stress–strain curves for the neat resin and nanocomposites are plotted in Fig. 6. The curves for the nanocomposites all show a reduced ductility, however, the increase in yield strength is sufficient to produce an overall tougher material; as toughness was calculated by the area under the stress–strain curve. The full dataset for the tensile tests is outlined in Table 3.

The tensile data for expanded graphite nanocomposites is included for comparison. Young's modulus, yield stress and strain to failure were obtained from the stress–strain plots, and toughness was calculated as the area under the stress–strain curve.

Significant increases in the nanocomposite strength and Young's modulus were observed on addition of 0.5 wt.% ATI functionalized graphite, to a stoichiometric ratio of epoxy components. The enhanced mechanical performance was attributed to the dispersion of the graphite nanoparticles into either individual sheets, or small aggregates of graphene sheets. Further benefits to strength and toughness were realized on increasing graphite loading to 1 wt.%. In this case, strength and Young's modulus were increased by 30% and 50%, respectively, relative to the base resin. At both the 0.5 wt.% and 1.0 wt.% loading, the trade-off in ductility and material toughness was small to negligible. It should be noted that similar levels of mechanical performance were not attained with EG nanocomposites. In this case, strength and Young's modulus was increased but ductility and toughness were considerably reduced. The reinforcement in this material was poorly dispersed and lacked surface functionality to allow load transfer from the matrix to the filler. Evidence of the graphite aggregation and poor interface in these materials was observed in the failed tensile specimens by SEM. A representative image is shown in Fig. 7. A SEM image of the surface of a failed tensile bar containing ATI graphite is shown for comparison. In that image, there is not evidence of large voids resulting from interfacial failure. The images suggest a greater degree of interfacial bonding in the ATI filled materials.

The marginal improvements to material properties of the samples containing excess amine may be due to the low degree of epoxy functionalization on the graphite. As the epoxy coverage consisted of only 4 wt.% epoxy, the added amine was unnecessary. As a result, there may have been excess amine plasticizing the system, which would account for the significant increase in nanocom-

Table 3
Stress–strain data.

Material	0.5 wt.% ATI graphite				1.0 wt.% ATI graphite			
	E (GPa)	σ_y (MPa)	$\varepsilon_{failure}$ (%)	Toughness (MPa)	E (GPa)	σ_y (MPa)	$\varepsilon_{failure}$ (%)	Toughness (MPa)
ATI functionalized graphite								
Neat resin	0.78 ± 0.04	17.7 ± 0.4	45 ± 8	875 ± 62	0.78 ± 0.04	17.7 ± 0.4	45 ± 8	875 ± 62
0% Excess amine	1.01 ± 0.06	21.2 ± 1.5	51 ± 4	896 ± 69	1.17 ± 0.01	23.1 ± 1.0	39 ± 1	779 ± 21
5% Excess amine	0.88 ± 0.01	20.3 ± 0.5	62 ± 3	1000 ± 34	0.76 ± 0.07	17.5 ± 0.4	60 ± 4	1055 ± 48
10% Excess amine	0.69 ± 0.06	17.9 ± 0.2	67 ± 4	1151 ± 34	0.81 ± 0.06	18.5 ± 0.5	63 ± 1	876 ± 14
Expanded graphite								
0.5 wt.%	1.19 ± 0.02	19.7 ± 1.4	20 ± 3	4 ± 0.4				
1.0 wt.%	1.49 ± 0.03	23.8 ± 0.8	3 ± 0	0.5 ± 0.3				
3.0 wt.%	1.83 ± 0.01	18.3 ± 0.1	2 ± 0	0.3 ± 0.1				

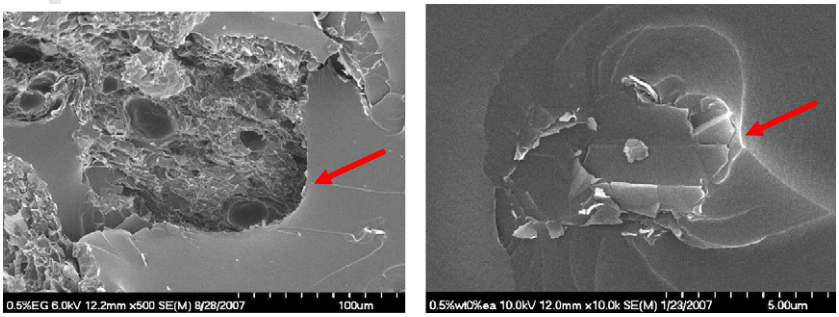

Fig. 7. SEM images of the surface of failed tensile specimens containing 0.5 wt.% EG (left), and 0.5 wt.% ATI, 0% excess amine (right).

Please cite this article in press as: Miller SG et al. Characterization of epoxy functionalized graphite nanoparticles and the physical properties of epoxy matrix nanocomposites. Compos Sci Technol (2010), doi:10.1016/j.compscitech.2010.02.023

Table 4
Glass transition temperatures of epoxy-ATI functionalized graphite nanocomposites.

ATI, 0% excess amine	T_g (°C)	ATI, 5% excess amine	T_g (°C)	ATI, 10% excess amine	T_g (°C)
0% graphite	34	0% graphite	34	0% graphite	34
0.5 wt.%	35	0.5 wt.%	32	0.5 wt.%	29
1.0 wt.% *amine*	33	1.0 wt.% *amine*	29	1.0 wt.%	29

posite toughness and ductility that was noted for these systems. A decrease in T_g within the nanocomposite containing excess amine was also observed, Table 4, suggesting the presence of unreacted low molecular weight material. Additional curing agent would have provided a means to ensure that the system was crosslinked; however, the additional curing agent was not necessary as suggested by the unimproved mechanical properties and the reduced glass transition temperature.

4. Conclusions

The unique feature of the ATI epoxy functionalized graphite which functionalized a portion of expanded graphite layers, provided improved particulate dispersion and material properties. The nanoparticle was well dispersed after only 15 min of stirring with the epoxy resin, and dispersion did not increase epoxy viscosity to the same extent as the unfunctionalized material, which benefits the processability of this material. The result of the partial functionalization was a five order of magnitude increase in electrical conductivity and a 30% and 50% improvement in strength and stiffness, respectively. A corresponding reduction in material toughness was not observed.

References

[1] Shim BS, Starkovich J, Kotov N. Multilayer composites from vapor-grown carbon nano-fibers. Compos Sci Technol 2006;66:1174–81.
[2] Bagwell RM, McManaman JM, Wetherhold RC. Short shaped copper fibers in an epoxy matrix: their role in a multifunctional composite. Compos Sci Technol 2006;66:522–30.
[3] Usuki A, Hasegawa N, Kato M. Polymer clay nanocomposites. Adv Polym Sci 2005;179:135–95.
[4] Krishnamoorti R, Yurekli K. Rheology of polymer layered silicate nanocomposites. Curr Opin Colloid Interface Sci 2001;6:464–70.
[5] Shi H, Lan T, Pinnavaia TJ. Interfacial effects on the reinforcement properties of polymer–organoclay nanocomposites. Chem Mater 1996;8:1584–7.
[6] Osorio AG, Silveira ICL, Bueno VL, Bergmann CP. $H_2SO_4/HNO_3/HCl$ – functionalization and its effect on dispersion of carbon nanotubes in aqueous media. Appl Surf Sci 2008;255:2485–9.
[7] Datsyuk V, Kalyva M, Papagelis K, Parthenios J, Tasis D, Siokou A, et al. Chemical oxidation of multiwalled carbon nanotubes. Carbon 2008;46(6):833–40.
[8] Bikiaris D, Vassiliou A, Chrissafis K, Paraskevopoulos KM, Jannakoudakis A, Docoslis A. Effect of acid treated multi-walled carbon nanotubes on the mechanical, permeability, thermal properties and thermo-oxidative stability of isotactic polypropylene. Polym Degrad Stabil 2008;93(5):952–67.
[9] Lafuente E, Callejas MA, Sainz R, Benito AM, Maser WK, Sanjuán ML, et al. The influence of single-walled carbon nanotube functionalization on the electronic properties of their polyaniline composites. Carbon 2008;46:1909–17.
[10] Salavati-Niasari M, Mirsattari SN, Bazarganipour M. Synthesis, characterization and catalytic oxyfunctionalization of cyclohexene with *tert*-butylhydroperoxide over a manganese(II) complex covalently anchored to multi-wall carbon nanotubes (MWNTs). Polyhedron 2008;18:3653–61.
[11] Chamssedine F, Claves D. Three different modes of fluorine chemisorption at the surface of single wall carbon nanotubes. Chem Phys Lett 2007;443(1–3):102–6.
[12] Liu YT, Zhao W, Huang ZY, Gao YF, Xie XM, Wang XH, et al. Noncovalent surface modification of carbon nanotubes for solubility in organic solvents. Carbon 2006;44(8):1613–6.
[13] Peng F, Pan F, Sun H, Lu L, Jiang Z. Novel nanocomposite pervaporation membranes composed of poly(vinyl alcohol) and chitosan-wrapped carbon nanotube. J Membrane Sci 2007;300(1–2):13–9.
[14] Stankovich S, Piner RD, Nguyen ST, Ruoff RS. Synthesis and exfoliation of isocyanate-treated graphene oxide nanoplatelets. Carbon 2006;44(15):3342–7.
[15] Ramanathan T, Abdala AA, Stankovich S, Dikin DA, Herrera-Alonso M, Piner RD, et al. Functionalized graphene sheets for polymer nanocomposites. Nat Nanotechnol 2008;3:327–31.
[16] Schniepp HC, Li JL, McAllister MJ, Sai H, Herrera-Alonso M, Adamson DH, et al. Functionalized single graphene sheets derived from splitting graphite oxide. J Phys Chem B 2006;110(17):8535–9.
[17] Kalaitzidou K, Fukushima H, Drzal LT. A new compounding method for exfoliated graphite–polypropylene nanocomposites with enhanced flexural properties and lower percolation threshold. Compos Sci Technol 2007;67(10):2045–51.
[18] Bartholome C, Miaudet P, Derré A, Maugey M, Roubeau O, Zakri C, et al. Influence of surface functionalization on the thermal and electrical properties of nanotube–PVA composites. Compos Sci Technol 2008;68(12):2568–73.
[19] Shenogin S, Bodapati A, Xue L, Ozisik R, Keblinski P. Effect of chemical functionalization on thermal transport of carbon nanotube composites. Appl Phys Lett 2004;85:2229.
[20] Ma PC, Kim JK, Tang BZ. Effects of silane functionalization on the properties of carbon nanotube/epoxy nanocomposites. Compos Sci Technol 2007;67(14):; 2965–2972.
[21] Yasmin A, Luo JJ, Daniel IM. Processing of expanded graphite reinforced polymer nanocomposites. Compos Sci Technol 2006;66:1182–9.
[22] Chen G, Wu C, Weng W, Wu D, Yan W. Preparation of polystyrene/graphite nanosheet composite. Polymer 2003;44(6):1781–4.
[23] Allred RE, Gosau JM, Barlow JP. Surface modification of exfoliated graphite nanoreinforcements. In: SAMPE 2006 fall technical conference, Dallas, TX.
[24] Allred RE, Gosau JM, Barlow JP, Miller SG. Adhesion and dispersion promoting treatments for graphite nanoflakes. In: SAMPE 2009 conference, Baltimore, MD.
[25] Littell JD, Ruggeri CR, Goldberg RK, Roberts GD, Arnold WA, Binienda WK. Measurement of epoxy resin tension, compression, and shear stress–strain curves over a wide range of strain rates using small test specimens. J Aerospace Eng 2008;21:162.
[26] Raghu AV, Lee YR, Jeong HM, Shin CM. Preparation and physical properties of waterborne polyurethane/functionalized graphene sheet nanocomposites. Macromol Chem Phys 2008;209:2487–93.
[27] Lee SH, Cho E, Jeon SH, Youn JR. Rheological and electrical properties of polypropylene composites containing functionalized multi-walled carbon nanotubes and compatibilizers. Carbon 2007;45:2810–22.
[28] Yu A, Ramesh P, Sun X, Bekyarova E, Itkis ME, Haddon RC. Enhanced thermal conductivity in a hybrid graphite nanoplatelet carbon nanotube filler for epoxy composites. Adv Mater 2008;20:4740–4.
[29] Bekyarova E, Itkis ME, Cabrera N, Zhao B, Yu A, Gao J, et al. Electronic properties of single-walled carbon nanotube networks. J Am Chem Soc 2005;127:5990–5.
[30] Dumitrescu I, Wilson NR, Macpherson J. Functionalizing single-walled carbon nanotube networks: Effect on electrical and electrochemical properties. J Phys Chem C 2007;111(35):12944–53.

Please cite this article in press as: Miller SG et al. Characterization of epoxy functionalized graphite nanoparticles and the physical properties of epoxy matrix nanocomposites. Compos Sci Technol (2010), doi:10.1016/j.compscitech.2010.02.023